

## Seasonal phytoplankton blooms associated with monsoonal influences and coastal environments in the sea areas either side of the Indochina Peninsula

Dan Ling Tang,<sup>1</sup> Hiroshi Kawamura,<sup>2</sup> Ping Shi,<sup>1</sup> Wataru Takahashi,<sup>3</sup> Lei Guan,<sup>4</sup> Teruhisa Shimada,<sup>2</sup> Futoki Sakaida,<sup>2</sup> and Osamu Isoguchi<sup>2</sup>

Received 3 May 2005; revised 1 November 2005; accepted 15 November 2005; published 17 February 2006.

[1] The Gulf of Thailand (GoT) is a semienclosed sea on the west and southwest side of the Indochina Peninsula and connects with the near-coastal waters of the South China Sea (SCS) on the east and northeast side of the Malay Peninsula. The objective of the present study is to understand dynamic features of the phytoplankton biology in the GoT and the nearby SCS, on both sides of the Indochina Peninsula, using remote-sensing measurements of chlorophyll-*a* (Chl *a*), sea surface temperature (SST), and surface vector winds obtained during the period from September 1997 to March 2003. Results show that seasonal variations of the phytoplankton blooms are primarily controlled by the monsoonal winds and related coastal environments. The GoT and the near-coastal SCS have a peak in the averaged monthly Chl *a* in December and January, which is associated with the winter northeaster monsoon. The near-coastal SCS have another big peak in the averaged monthly Chl *a* in summer (July to September), which is associated with the summer southwest monsoon. The offshore bloom in the GoT occurs in its southern part and enhances the December–January peak of averaged monthly Chl *a*. By contrast, the offshore bloom in the nearby SCS is observed northeast of the Peninsula, and represents the primary source of the July–September peak Chl *a*. Here the coastal upwelling associated with the offshore Ekman transport caused by the coastal surface winds parallel to the Vietnam east coast gives physical conditions favorable to the development of offshore phytoplankton blooms. The Mekong River discharge waters flow in different directions, depending on the monsoon winds, and contributes to seasonal blooms on both sides of the Peninsula.

**Citation:** Tang, D. L., H. Kawamura, P. Shi, W. Takahashi, L. Guan, T. Shimada, F. Sakaida, and O. Isoguchi (2006), Seasonal phytoplankton blooms associated with monsoonal influences and coastal environments in the sea areas either side of the Indochina Peninsula, *J. Geophys. Res.*, *111*, G01010, doi:10.1029/2005JG000050.

### 1. Introduction

[2] The Gulf of Thailand (GoT) is a semienclosed sea defined by the Malay Peninsula and by the Indochina Peninsula (IP). The GoT is on the west and southwest side of the IP and the western South China Sea (SCS) is on the east and northeast side of the IP (Figure 1). In the present study, we compare biological and oceanic conditions between the GoT and the nearby western SCS in two sides of the IP using satellite measurements.

[3] The human population in the coastal zone of GoT is large and its rapid economic growth is continuing, and the GoT is a major and rapidly developing commercial fishing area, as well. Although the eastern waters of the GoT and those of the western SCS connect with each other at around the tip of the IP, and along the full length of the access to the GoT, previous studies on both sides of the Peninsula have been conducted separately, especially in the field of phytoplankton biology. Characteristics of chlorophyll-*a* (Chl *a*) and its biomass distribution, and the oceanic conditions associated with algal blooms, have not yet been clarified [Wyrki, 1961; Saadon *et al.*, 1999; Yanagi *et al.*, 2001].

[4] The Southeast Asian Fisheries Development Center (SEAFDEC) Training Department and the Marine Fishery Resources Development and Management Department (MFRDMD) jointly launched an Inter-Departmental Collaborative Research Program (IDCRP) in 1995 [Saadon *et al.*, 1999]. Oceanographic, environmental and marine biological studies were also conducted on M.V. SEAFDEC research cruises in September 1995 and April 1996. The research showed that the variability of physical properties in

<sup>1</sup>Laboratory for Tropical Marine Environmental Dynamics, South Chinese Sea Institute of Oceanology, Chinese Academy of Sciences, Guangzhou, China.

<sup>2</sup>Center for Atmospheric and Oceanic Studies, Graduate School of Science, Tohoku University, Sendai, Japan.

<sup>3</sup>Japan NUS Co., LTD, Tokyo, Japan.

<sup>4</sup>Ocean Remote Sensing Institute, Ocean University of China, Qingdao, China.

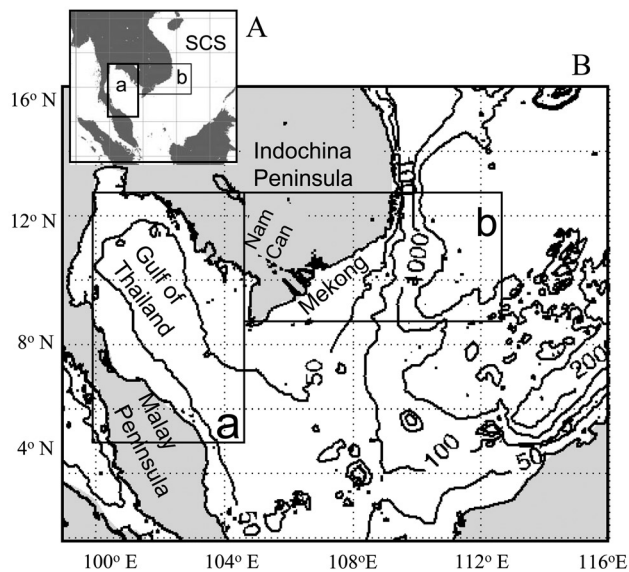


**Figure 1.** (a) Locations of study area. (b) Bathymetry and geography of study area around the Indochina Peninsula. Two boxes show the subregions in two sides of the Peninsula: area a, the Gulf of Thailand (GoT); area b, the nearby South China Sea (SCS).

the GoT and of coastal areas along the east coast of the Malay Peninsula could be correlated with the incidence and direction of monsoon winds in that region [Saadon *et al.*, 1999]. However, these research cruises were limited to the waters of the western GoT. Therefore, we lack result to allow comparison of the oceanic conditions of the GoT with the western SCS for the same times. The detailed characteristics in monthly oceanic variations of these two areas have not yet been clarified [Yanagi *et al.*, 2001]. The physical oceanographic data are too sparse (especially for the SCS near the east coast of the IP) to make a valid comparison of the variability of physical properties associated with different monsoonal wind conditions [Saadon *et al.*, 1999].

[5] Physical, chemical and biological processes are intimately linked in the ocean [Chaturvedi *et al.*, 1998; Tang *et al.*, 2004a, 2004b]. Chl *a* concentration, an index of phytoplankton biomass, is an important indicator of changing conditions in the marine ecosystem. Our studies on Harmful Algal Blooms (HABs) in the western SCS [Tang *et al.*, 2004a] have shown that HABs frequently occur in the waters off the east coast of Vietnam during the southwest monsoon season. In contrast, HABs were observed in the Rach Gia Bay in the GoT during the northeast monsoon season. These preliminary observations have indicated differences between the conditions of the GoT and the near-coastal SCS on either side of the IP (Figure 1).

[6] Recently, a series of papers have revealed characteristic features of air-sea-land interactions in the seas around the pit of Indian and east coast of Vietnam, among various types of coastal dynamics [Luis and Kawamura, 2000, 2002a, 2002b; Tang *et al.*, 2003, 2004a, 2004b]. These researchers mainly used remotely sensed parameters for examining phenomena of interests, and combined a numerical physical ocean model for understanding of results. In

the present study, relationships between phytoplankton blooms and the ocean dynamics around the tip of the Peninsula are examined using satellite data on Chl *a*, SST and surface winds as a first step toward a better understanding of the dynamic features of the phytoplankton biology in the seas on both sides of the IP.

## 2. Study Area, Satellite Data, and Methods

### 2.1. Study Area

[7] The study area includes part of the western SCS (b, Figure 1) (the nearby SCS) and the GoT (area a, Figure 1), which are on either side of the IP. The “toe-shaped” coastline of the Peninsula protrudes southeastward from the Nam Can. The average depth of GoT is about 40 m, shallower than that of the nearby SCS. This region experiences the reversed wind system of the Asian monsoon [Shaw and Chao, 1994] that play important roles in the hydrological features and water circulation in this region [Wyrski, 1961].

[8] The study regions are more precisely defined as the GoT (area a in Figure 1, 100°E–104°E, 6°N–12°N) and the nearby SCS (area b in Figure 1, 104°E–108°E, 2°N–10°N). The GoT receives fresh-water discharges from eleven rivers [Snidvongs, 1998] while the nearby SCS receives a large volume of fresh-water discharge from the Mekong River. The discharges have a strong seasonality associated with the monsoon, and are enhanced in June–September (<http://www.sage.wisc.edu/riverdata>).

### 2.2. Satellite-Derived Chl *a*

[9] SeaWiFS measurements were processed using the Ocean Color 4-band algorithm (OC4) [O’Reilly *et al.*, 1998, 2000] with the SeaWiFS Data Analysis System (SeaDAS). Monthly mean Chl *a* images with 3 km × 3 km spatial resolution were obtained and processed for the study area. The SeaWiFS data accumulated in the Asian I-Lac database [Tang *et al.*, 2002] represent about 2700 scenes for the GoT and about 1700 scenes for the nearby SCS. Ocean Color and Temperature Scanner (OCTS) aboard ADEOS-I provided the satellite-derived Chl *a* data, with quality similar to that of SeaWiFS for October 1996 to June 1997 [Kawamura and OCTS Team, 1998].

[10] Previous studies [Tang *et al.*, 2003, 2004b] show that SeaWiFS-derived Chl *a* values match survey measurement in most area in the western SCS, including coastal waters, but SeaWiFS Chl *a* values are higher than survey measurements near the Mekong River mouth.

### 2.3. Satellite-Derived Surface Vector Winds

[11] Ocean surface vector winds have been retrieved from measurements of the microwave scatterometers [e.g., Wentz *et al.*, 2001]. We used 0.5-degree graded monthly mean wind fields obtained from QuikSCAT observations for August 1999 to January 2004. ERS scatterometers with temporal resolution lower and swath coverage narrower than those of QuickSCAT have been operated for an even longer time, and this allowed extension of the monthly wind records for covering the SeaWiFS operation period. Therefore one-degree gridded monthly mean wind fields were used from the ERS scatterometer observations for January 1997 to July 1999. Both data sets are available at

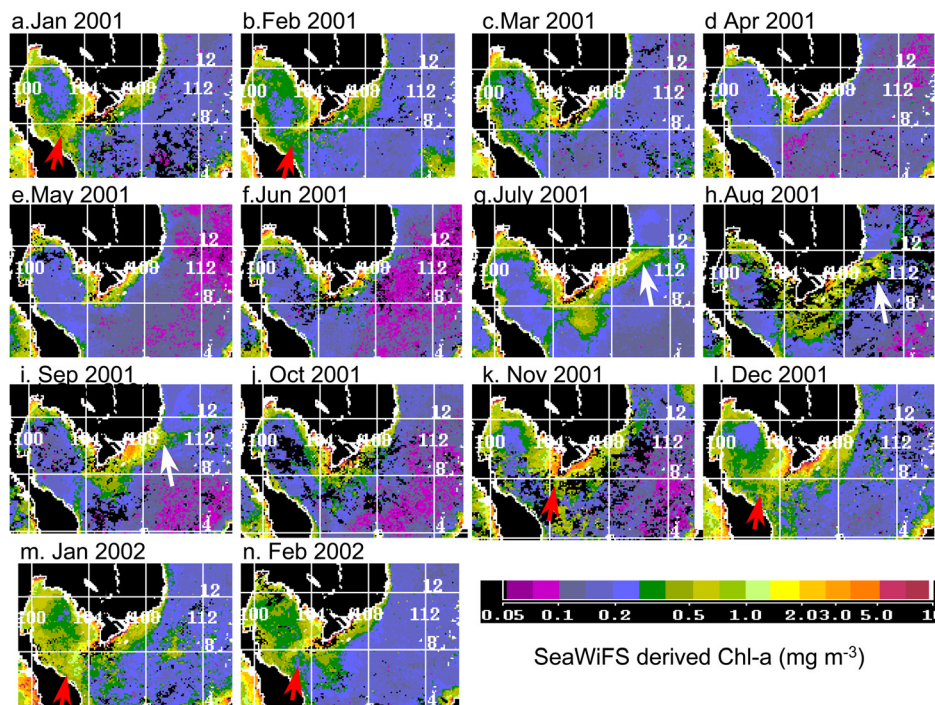


**Figure 2.** SeaWiFS-derived monthly Chl *a* images for 2001 and 2002. Red arrows and white arrows indicate the offshore blooms phenomena.

IFREMER/CERSAT [<http://www.ifremer.fr/cersat/en/data/gridded.htm>].

#### 2.4. MODIS-Derived SST and Chl *a*

[12] MODIS (Moderate Resolution Imaging Spectroradiometer) is a visible and infrared radiometer aboard the Terra (EOS AM) and Aqua (EOS PM) satellites. The Terra MODIS and Aqua MODIS observe the entire Earth's surface every 1 to 2 days. The version 4.1 level 3, 4-km mapped monthly sea surface temperature (SST) and Chl *a* concentration products (<http://modis.gsfc.nasa.gov/>) have been used in this study. SST products were derived by the Non-Linear (NLSST) algorithm [Walton *et al.*, 1998]. The Chl *a* concentration products were estimated by the semi-analytical algorithm.

#### 2.5. SeaWiFS-Derived Turbid Flag

[13] In order to examine influence of the river sediment, we analyze the SeaWiFS Turbid Flag (TF) and nLw 555 images for 1997–2003. Monthly images of the turbid flag appearance times for each pixel and monthly mean of the nLw 555 were calculated and integrated for the summer (June–August) and winter (December–February) monsoon seasons.

### 3. Results

#### 3.1. Chl *a* Distributions and Phytoplankton Blooms

[14] Figure 2 shows SeaWiFS-derived monthly Chl *a* distribution in 2001 and 2002. In general, Chl *a* concentration in the GoT was higher than that in the nearby SCS. The phytoplankton blooms with high Chl *a* concentrations ( $>1 \text{ mg m}^{-3}$ ) appeared in the offshore region southwest of the IP tip from November to February (red

arrows in Figures 2a, 2b, 2k, 2l, 2m and 2n). In the nearby SCS, Chl *a* concentrations were usually low ( $<0.5 \text{ mg m}^{-3}$ ), throughout the year. However, strong blooms, with a jet-like shape, were observed to the northeast of the Peninsula tip during July to September (white arrows in Figures 2g, 2h and 2i) [Tang *et al.*, 2004b]. In the coastal zones, on both sides of the IP tip, Chl *a* concentration was generally high throughout the year, but was further enhanced during the strong winds of the northeast monsoon season of November–February and the southwest monsoon season of July–September. Sediment contamination, which is shown in black color in Chl *a* images (Figure 2a), may be high near the Peninsula tip.

[15] Figure 3 indicates the monthly Chl *a* distributions in December 1996, June 1997 (OCTS), January 2001 and July 2001 (MODIS) derived from satellite ocean color sensors other than SeaWiFS. The December 1996 images (OCTS, Figure 3a) and January 2001 (MODIS, Figure 3c) illustrate the offshore blooms extending from the IP tip and the coastal blooms around the Mekong River mouth. The July 2001 image (MODIS, Figure 3d) is equivalent to the SeaWiFS Chl *a* distribution in Figure 2g. The jet-stream-like shape of the bloom in the nearby SCS is also visible in Figure 3d (white arrow). Because of ADEOS-I failure in June 1997, the monthly distribution of June 1997 is shown in Figure 3c instead of the July image. The offshore regions are masked by clouds, but the near-coastal features at around the Peninsula tip are similar to those of Figure 2f (June of 2001).

[16] In order to compare the Chl *a* distributions in the GoT with the nearby SCS, time series of areal averaged Chl *a* derived from SeaWiFS were produced for areas a and b in Figure 1 for the period from July 1999 to March 2003. Figure 4 shows the time series produced for GoT and the nearby SCS, which exhibit clear seasonal variations. For the GoT, there is one peak in December or January every

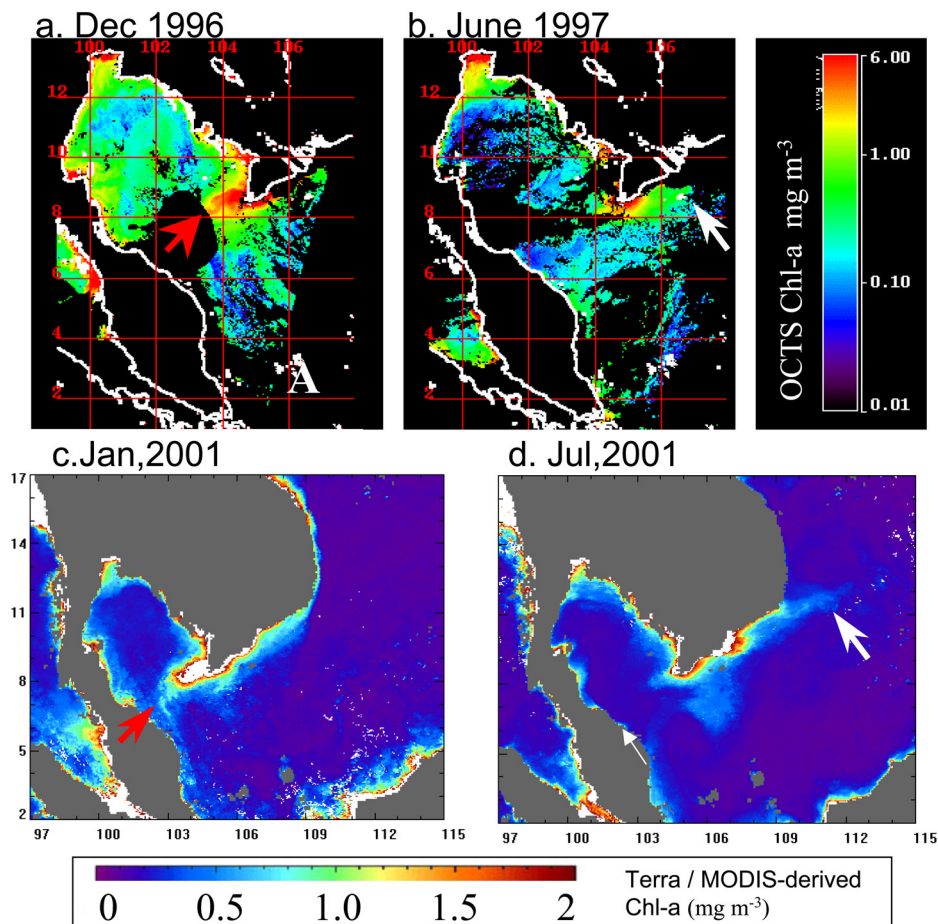


**Figure 3.** Monthly Chl *a* images derived from OCTS and MODIS.

year. Two peaks are seen in a year for the SCS; one peak is in December and another higher peak is around August. An obvious bloom is observed in December 1999 in the GoT (Figure 4a), and a longer intense bloom for July to September 2001 in the nearby SCS (Figure 4b).

[17] The seasonal variations of Chl *a* concentration (derived from SeaWiFS) in Figure 5 were obtained by integrating the monthly averaged Chl *a* concentrations shown in Figure 4. Figure 5 clearly demonstrates that there is one dominant December–January peak in the GoT with a possible secondary June–August peak, while there are two peaks, of December–January and July–September, in the nearby SCS.

### 3.2. Conditions of Surface Winds and Sea Surface Temperature (SST)

[18] Figure 6 shows monthly averaged surface vector winds in January, April, July and November 2001. The regional wind condition is dominated by the Asian monsoon, which alternates the wind direction in a year. In January of the winter monsoon peak (Figure 6a), strong northeasterly winds of about  $10 \text{ m s}^{-1}$  parallel the Vietnam coastline in the western SCS, and then change to weak easterly winds of about  $2 \text{ m s}^{-1}$  in the GoT. In July, at the time of the summer monsoon peak (Figure 6c), strong southwesterly winds hit the GoT-side coastline of the IP and again parallel the Vietnam coastline in the western SCS,

but in the opposite direction to that of January. However, in the southern area of the GoT, the winds are weaker and, near the mouth of the Gulf, gradually become strong toward the north. April (Figure 6b) is in between the monsoon peaks, and its wind condition is differs from that of the peak conditions. November (Figure 6d) represents the beginning of the winter monsoon, and, compared with January, the surface wind patterns are similar in the SCS, but differ in the GoT, perhaps as a result of the large-scale atmospheric pressure and vertical condition in the winter season.

[19] In addition, the Vietnam Current (also called the Sunda Slope Current) is the southward continuation of the Vietnam coastal current, due to the winter cyclonic wind curl in winter [Liu *et al.*, 2004]. This may contribute to the low SST signal of SCS observed in winter (January 2001, Figure 7a). Figure 6 clearly shows the seasonal wind conditions are different for the GoT from what they are for the nearby SCS.

[20] In January 2001 (Figure 7a), SST in the GoT was obviously higher than that in the nearby SCS. There is an extensive area of lower SST in the nearby SCS off the Vietnam coasts and in the southeast of the GoT. In April (figure is not shown), SST increases in the whole area up to about  $25^\circ\text{C}$ , and SST in the GoT is still higher than that in the nearby SCS. In July (Figure 7b), SST in the study area is rather uniform, but a lower SST region is observed in the Vietnam coastal sea (red arrow) and offshore in the SCS. In

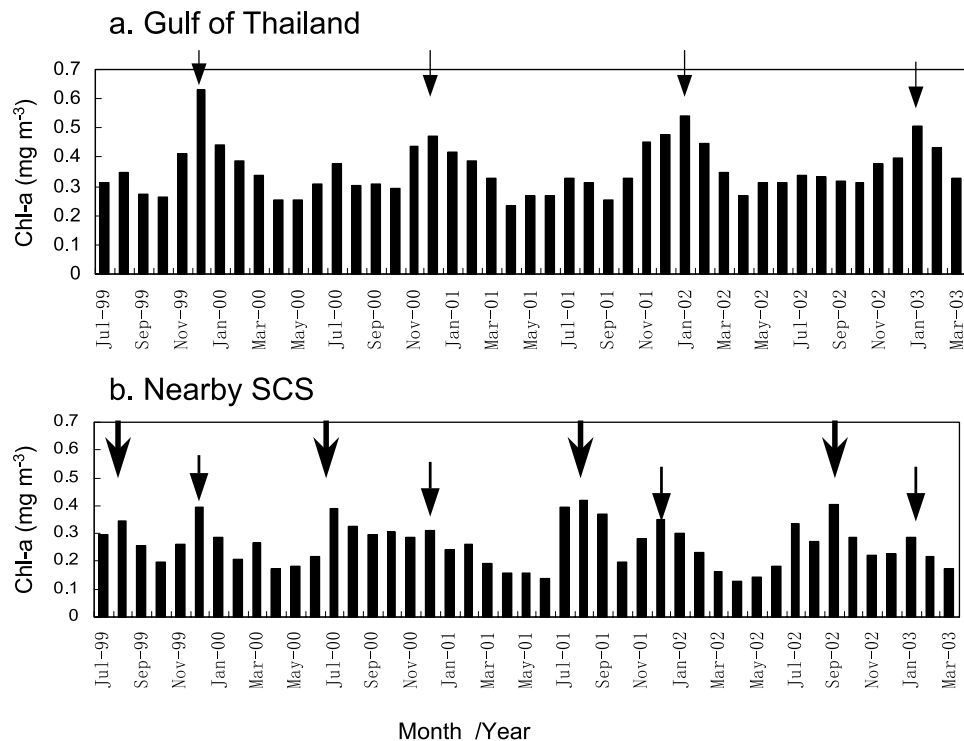


**Figure 4.** Time series of monthly Chl *a* concentrations (derived from SeaWiFS) in the subregions (areas a and b in Figure 1) during July 1999 to March 2003.

December (figure is not shown), the SST starts to decrease and lower SST regions appear along the Vietnam coast.

### 3.3. Mekong River Sediment Load

[21] Though we investigate the offshore phytoplankton blooms on both sides of the IP, there is a possibility that the satellite-derived Chl *a* may be influenced by the Mekong River sediment load. It is known that nLw555 is quite sensitive to the surface suspended sediment and used for its retrievals in various sea/estuary regions (e.g., Yellow Sea by *Ahn et al.* [2001]; Barents Sea by *Burenkov et al.* [2001]; Loire Estuary by *Doxran and Froidefond* [2003]), and it is confirmed that the nLw555 images show coastal behaviors similar to those of the turbid flag.

[22] As seen in the Figure 8a, the turbid flag appearance time is high (higher than 60) in the coastal region off the Mekong River. Sharp gradients of the appearance time between 40 and 60 make edges of the coastal high turbid flag-appearance regions in both monsoon seasons. When we consider the contour of 40 times as a boundary that affected by the Mekong sediment load, the offshore phytoplankton blooms (Figure 2 and 3) is far offshore from the turbid flag 40 line, particularly for summer season in the nearby SCS (Figure 8b).

## 4. Discussion

### 4.1. Hydrographical Conditions in the Gulf of Thailand

[23] The northeast wind prevails from November to March over the nearby SCS and the GoT and the southwest wind prevails from May to September [*Morgan and Valencia*, 1983]. The monsoon modifies climate, and influences

water-current speed and direction of water above the pycnocline at around a depth of 40 m and the surface currents in the nearby SCS [*Stansfield and Garrett*, 1997; *Snidvongs and Sojisuporn*, 1999]. During November–March, when the northeast monsoon dominates in the study area (Figure 6d), vertically well-mixed conditions are developed in the GoT [*Yanagi et al.*, 2001]. Because of the resultant nutrient transfer to the surface layer and favorable temperatures of about 27°–28°C (Figure 7a), phytoplankton grow well in the GoT (Figures 2a, 2b, 2c, 2k, 2l, 2m and 2n).

[24] Stratification of the water column in the GoT mostly develops in March–May between the two monsoon seasons

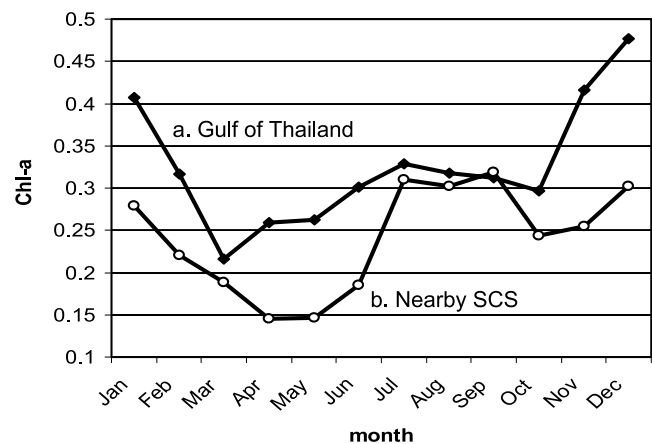


**Figure 5.** SeaWiFS-derived monthly Chl *a* concentrations in two subregions (areas a and b in Figure 1) averaged from July 1999 to March 2003.

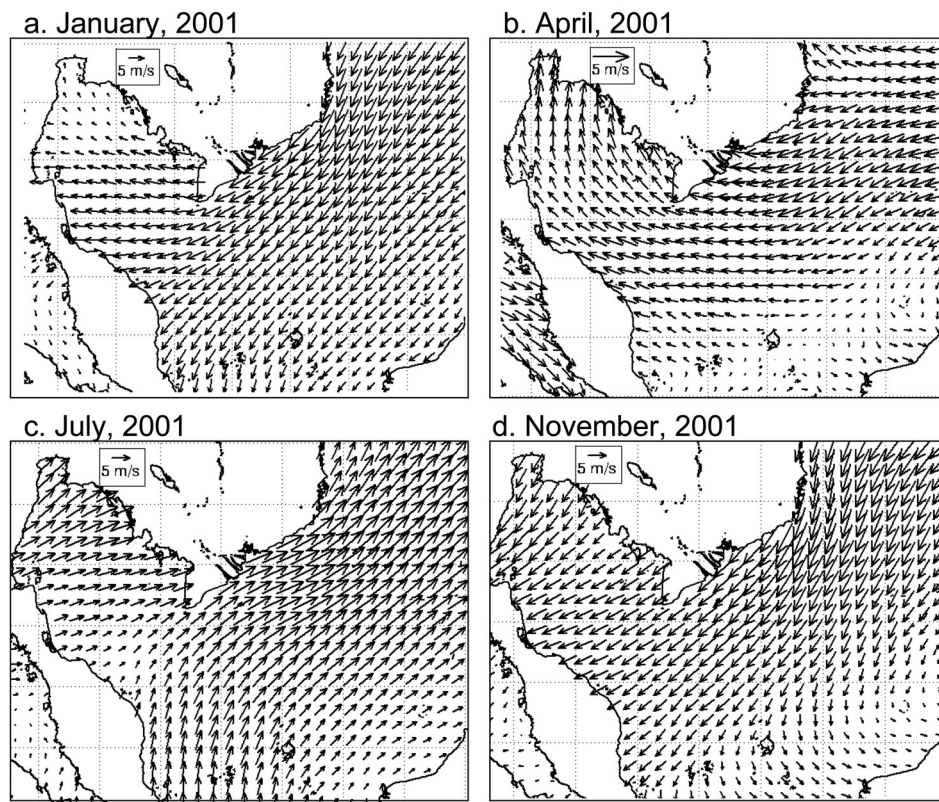


**Figure 6.** Monthly mean QuikScat surface vector winds for (a) January, (b) April, (c) July, and (d) November 2001.

that is mainly due to significant sea surface heating and weak sea surface winds in this season (Figure 6b). The low Chl *a* concentrations of the GoT for May–June (Figures 2e and 2f) are considered to be associated with the well-developed surface stratification. The stratification is weakened during September–October and vanishes in December–January [Morgan and Valencia, 1983; Yanagi *et al.*, 2001]. SSTs start to increase and become uniform in July (Figure 7b) while the southwest monsoon prevails [Saadon *et al.*, 1999]. These seasonal hydrographical conditions can be the primary reason for the seasonal changes of Chl *a* (Figure 4). The Chl *a* peak enhanced by the additional offshore blooms phenomena will be discussed in section 4.2.

#### 4.2. Phytoplankton Blooms and Oceanic Conditions in the GoT and Nearby SCS

[25] Water conditions may result in phytoplankton blooms and, therefore, a defined area of increased Chl *a* concentration [Tang *et al.*, 1998, 1999, 2002]. Characteristics of the regional Chl *a* and biomass distributions and of the regional oceanic conditions have not yet been clarified in the GoT and the near by SCS [Wyrski, 1961; Saadon *et al.*, 1999; Yanagi *et al.*, 2001].

##### 4.2.1. Previous Studies Using in Situ Observations

[26] *Rojana-anawat and Snidvongs* [1999] reported some evidence that intermediate waters in the nearby SCS might flow into the GoT along the central axis and coast of Vietnam and Cambodia, and exit from the Gulf along the Thai-Malay coast of the Malay Peninsula. In March–May, water exchange between the GoT and the nearby SCS becomes

large owing to a coupled effect of the intensified estuarine circulation and the Ekman transport by the summer monsoon [Yanagi *et al.*, 2001]. During June–September, the water in the upper 10 m flows to the GoT [Saadon *et al.*, 1999].

[27] Previous studies using in situ measurements have reported blooms of the blue-green algae, *Microcystis* sp., in Rach Gia Bay in December 2002 [Nguyen *et al.*, 2003] and occurring HABs along the east coast waters of Vietnam in the summer southwesterly monsoon season [Tang *et al.*, 2004a].

##### 4.2.2. The Present Study

[28] Phytoplankton blooms have been observed on both sides of the IP, using long-term data sets of satellite observations, which provide monthly high-resolution distributions of Chl *a* (Figures 2 and 3), surface vector winds (Figure 6) and SST (Figure 7). We summarize those features in Table 1.

[29] The seasonal variations in phytoplankton blooms are primarily controlled by the monsoon winds. The GoT and the nearby SCS have a peak of monthly Chl *a* in December–January (Figure 5), which is associated with the winter monsoon. In the winter season (December–January), sea surface waters cooling and mechanical mixing cause active convection in the sea surface layer and transfer subsurface nutrients to the euphotic zone.

[30] The Chl *a* concentration in the coastal zone is generally high throughout the year. Responses of the coastal zone waters to the monsoonal winds are similar in both GoT and nearby SCS, but are more enhanced in the GoT (Figures 4 and 5). The GoT's shallower depth and accumulated nutrients

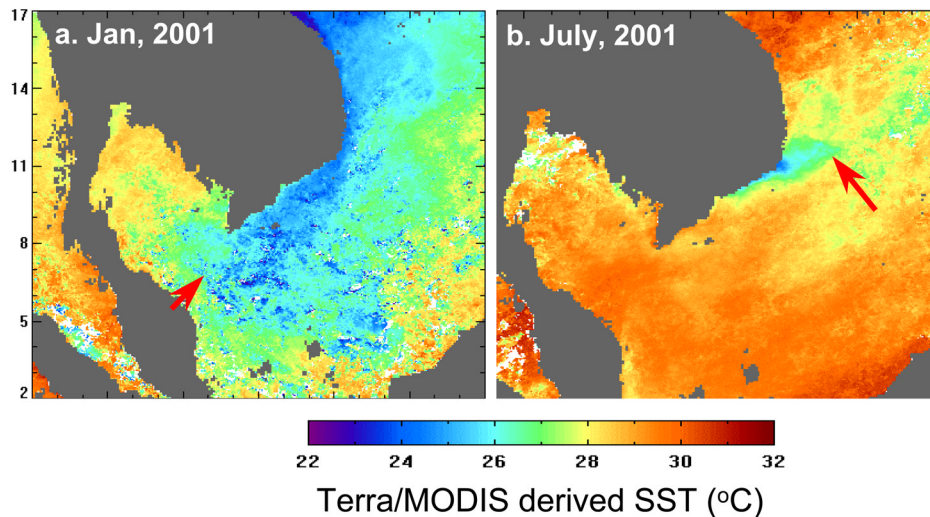


**Figure 7.** MODIS derived monthly mean SST images for (a) January and (b) July 2001.

in the subsurface are significant characteristics in this monsoon-enhanced nutrient transfer. As seen in Figure 5, the resulting enhanced algal blooms contribute to the winter peak (December–January) and the summer (July–September) peak in the GoT and a rise around July in the nearby SCS. It is not clear from the present study whether or not the recent eutrophication due to the regional economical developments enhances the seasonal blooming in the GoT.

[31] The distinctive features in the study area are the offshore phytoplankton blooms (Table 1), in the GoT during the winter northeast monsoon (red arrows in Figures 2a, 2b, 2l, 2m, and 2n) and in the nearby SCS during the southwest monsoon (white arrows in Figures 2g, 2h, and 2i). These are schematically illustrated in Figure 9.

[32] The offshore bloom in the GoT occurs in the southeastern part of region a (a in Figure 1) and enhances the December peak of monthly Chl *a* (Figure 5). By contrast, the offshore bloom in the nearby SCS is observed in the northeastern part of region b (b in Figure 1a) and becomes the primary reason for the July–September peak in Chl *a* (Figure 5).

[33] In addition, the Mekong River fresh-water discharge, rich in nutrients, also enhances the seasonal phytoplankton blooms on both sides of the IP. During the winter northeast

monsoon season, the Mekong River plume flows to the south, and into the GoT, allowing the nutrients to enhance the winter bloom. In the summer southwestern monsoon season, however, the wind, upwelling forcing and subsequent geostrophic adjustment are reversed; the river discharge is high in this season and the nutrients enhance the summer bloom in the nearby SCS on the east side of the Peninsula.

#### 4.2.3. Proposed Physical Mechanisms to Explain the Offshore Phytoplankton Blooms

[34] The offshore phytoplankton blooms in the nearby SCS have been investigated by *Tang et al.* [2004a] to reveal that the strong surface winds parallel to the Vietnam east coast (Figure 9b) were the primary force to generate the offshore currents through the Ekman dynamics. Further north, along the coastline of Binh Thuan Province (BTP in Figure 9), the slope of the continental shelf is steep down to a depth of 2000 m, and deeper cooler water is upwelled to the surface layer (coastal upwelling) [*Tang et al.*, 2004a].

[35] The winter monsoon cools the ocean surface waters and develops mixed layers in the GoT, which results in the wider low SST in the nearby SCS (Figure 7a). The northeast winds parallel to the Vietnam east coast result in Ekman transport toward the shore and cause sea level rise in the

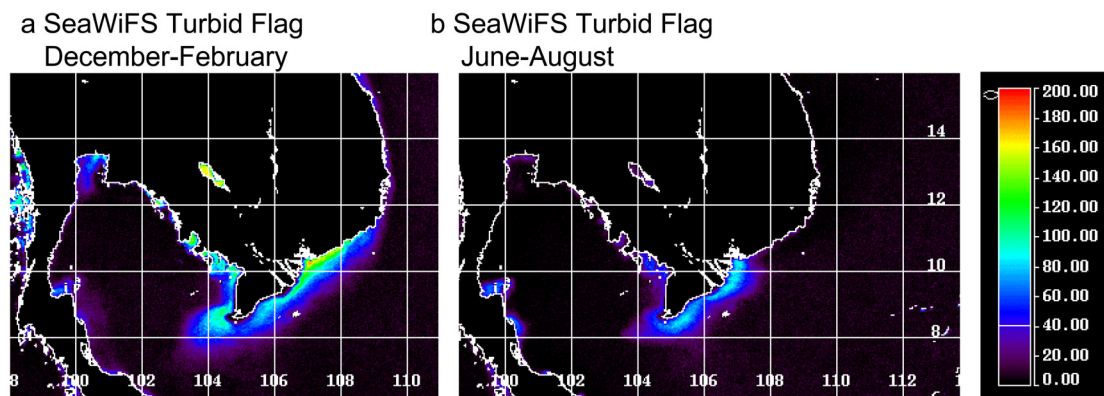


**Figure 8.** SeaWiFS derived turbid flag (TF) for (a) winter and (b) summer.

**Table 1.** Comparison of Phytoplankton Blooms and Environmental Conditions Between GoT and the Nearby South China Sea (SCS) in Two Sides of Indochina Peninsula<sup>a</sup>

Features	GoT	Nearby SCS
	<i>General Parameters</i>	
Region (Figure 1)	west side of the IP (area a in Figure 1)	east side of the IP (area b in Figure 1)
Regionally averaged monthly Chl <i>a</i> , mg/m <sup>3</sup>		
Range (Figure 4)	0.25–0.6 (Figure 4a)	0.1–0.4, 0.2 (Figure 4b)
Peaks (Figure 4 and 5)	one peak: December–January	two peaks: December–January, August
	<i>Distribution of Chl <i>a</i> in Coastal Zone (Both Sides) of the Indochina Peninsula</i>	
Common features (Figure 2 and 3)	generally high throughout the year enhanced during the monsoon season	same as for GoT.
Example of HABs	Rach Gia Bay, December 2002	Phan Ri Bay, August 2002
Mekong River fresh-water discharge	flow to GoT side during winter northeast monsoon season (Figure 9a)	flow to SCS side during summer southwest monsoon season (Figure 9b)
	<i>Offshore Phytoplankton Bloom</i>	
Season	November to February	July to September
Locations of phytoplankton blooms (Figure 2 and 3)	southwest of the IP tip (red arrows in Figure 2)	northeast of the IP tip (white arrows in Figure 2)
Surface vector wind conditions (Figure 6)	northeast wind parallel to the west coast of the IP	southwest wind parallel to the east coast of the IP
SST (Figure 7)	wider SST cooling in the southeast of GoT	uniform SST with low SST in the Vietnam coastal water and offshore region

<sup>a</sup>IP, Indochine Peninsula.

coastal regions of southeast Vietnam (Figure 9a). Balancing against to the Coriolis force, the coastal sea level rise forms a coastal-trapped alongshore current, i.e., a coastal jet stream, toward the Peninsula tip [Csanady, 1982; Unoki, 1993]. Around the tip, the coastal jet stream in rich nutrients becomes free from the right sidewall of the coastline and results in an offshore bloom in the open sea.

[36] The proposed physical mechanisms are simplified and need further research. A detailed discussion on the dynamics between the Vietnam coastal land topography and the atmospheric boundary layer is beyond the scope of present study.

## 5. Summary

[37] 1. Seasonal variations of the occurrence and location of phytoplankton blooms are primarily controlled by the monsoon winds.

[38] 2. The major offshore phytoplankton blooms appear in the GoT during the winter northeast monsoon season. In contrast, the offshore phytoplankton blooms in the nearby SCS occur during the summer southwest monsoon season.

[39] 3. The coastal upwelling associated with the offshore-ward Ekman transport in summer, derived from the southwest coastal surface winds parallel to the Vietnam eastern coast; it is favorable for the offshore phytoplankton bloom in the nearby SCS.

[40] 4. The southward current along the Vietnam east coast advects the cool water with high concentrations of nutrients to the GoT, released from the coastline around the Peninsula tip; it is favorable for the winter offshore phytoplankton bloom in the GoT.

[41] 5. Seasonal changes in river discharges forced by monsoon winds also enhance phytoplankton blooms in the GoT during the winter northeasterly monsoon season and in

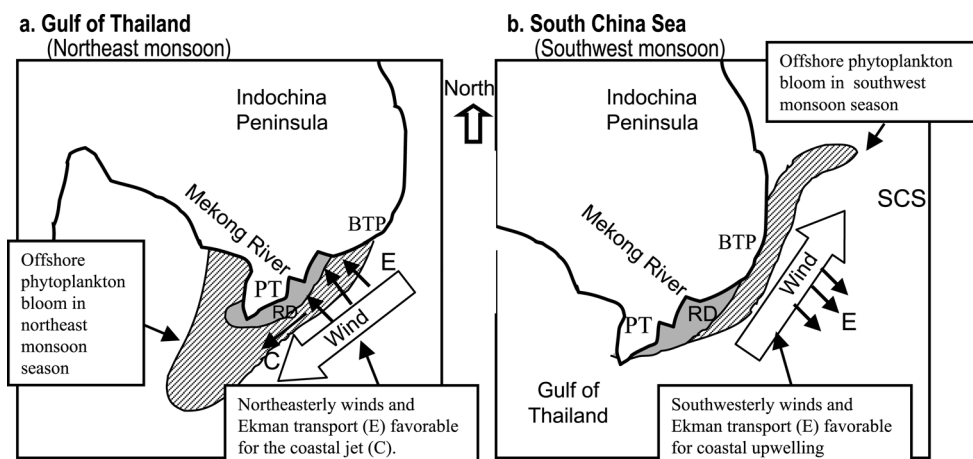


**Figure 9.** Schematic pictures of phytoplankton blooms on the two sides of the Indochina Peninsula. RD denotes river discharge.

the nearby SCS during the summer southwesterly monsoon season.

[42] **Acknowledgments.** This work was jointly supported by a Research Program of Chinese Academy of Sciences (KZCX3-SW-227-3), National Natural Science Foundation of China (40576053), and “One Hundred Talents Program of Chinese Academy of Sciences” awarded to DanLing Tang, and “Red-Tide Watcher” of the Special Coordination Fund for Promoting Science and Technology, Ministry of Education, Culture, Sports, Science and Technology, Japan. The authors greatly appreciate Joe Baker of Office of Chief Scientist, DPI, Queensland, Australia, for his valuable help on this study.

## References

- Ahn, Y. H., J. E. Moon, and S. Gallegos (2001), Development of suspended particulate matter algorithms for ocean color remote sensing, *Korean J. Remote Sens.*, *17*(4), 285–295.
- Burenkov, V. I., S. V. Ershova, O. V. Kopelevich, S. V. Sheberstov, and V. P. Shevchenko (2001), An estimate of the distribution of suspended matter in the Barents Sea waters on the basis of the SeaWiFS satellite ocean color scanner, *Oceanology*, *41*(5), 622–628.
- Chaturvedi, N., A. Narain, and P. C. Pandey (1998), Phytoplankton pigment/temperature relationship in the Arabian Sea, *Indian J. Mar. Sci.*, *27*, 286–291.
- Csanady, G. T. (1982), *Circulation in the Coastal Ocean*, 279 pp., Springer, New York.
- Doxran, D., and J. M. Froidefond (2003), Remote-sensing reflectance of turbid sediment-dominated waters: Reduction of sediment type variations and changing illumination conditions effects by use of reflectance ratios, *Appl. Opt.*, *42*(15), 2623–2634.
- Kawamura, H., and OCTS Team (1998), OCTS mission overview, *J. Oceanogr.*, *54*, 383–399.
- Liu, Q. Y., J. Xia, S. P. Xie, and W. T. Liu (2004), A gap in the Indo-Pacific warm pool over the South China Sea in boreal winter: Seasonal development and interannual variability, *J. Geophys. Res.*, *109*, C07012, doi:10.1029/2003JC002179.
- Luis, A. J., and H. Kawamura (2000), Wintertime wind forcing and sea surface cooling near the south India tip observed using NSCAT and AVHRR, *Remote Sens. Environ.*, *73*, 55–64.
- Luis, A. J., and H. Kawamura (2002a), A case study of sea surface temperature-cooling dynamics near the Indian tip during May 1997, *J. Geophys. Res.*, *107*(C10), 3171, doi:10.1029/2000JC000778.
- Luis, A. J., and H. Kawamura (2002b), Dynamics and mechanism for sea surface cooling near the Indian tip during winter monsoon, *J. Geophys. Res.*, *107*(C11), 3187, doi:10.1029/2000JC000455.
- Morgan, J. R., and M. J. Valencia (1983), The natural environmental setting, in *Atlas for Marine Policy in Southeast Asian Seas*, edited by J. R. Morgan and M. J. Valencia, pp. 4–17, Univ. of Calif. Press, Berkeley.
- Nguyen, N. L., N. H. Doan, T. M. A. Nguyen, and V. T. Ho (2003), A summary of HAB studies in Vietnam, paper presented at Workshop on Red Tide Monitoring in Asian Coastal Waters, Univ. of Tokyo.
- O’Reilly, J. E., S. Maritorena, B. G. Mitchell, D. A. Siegel, K. L. Carder, S. A. Garver, M. Kahru, and C. McClain (1998), Ocean color chlorophyll algorithms for SeaWiFS, *J. Geophys. Res.*, *103*, 24,937–24,953.
- O’Reilly, J. E., et al. (2000), Ocean color chlorophyll algorithms for SeaWiFS, OC2, and OC4: Version 4, in *SeaWiFS Postlaunch Calibration and Validation Analyses: Part 3*, edited by S. B. Hooker and E. R. Firestone, *NASA Tech. Memo.*, 2000-206892(11), 9–23.
- Rojana-anawat, P., and A. Snidvongs (1999), Dissolved oxygen and carbonate-carbon dioxide in the sea water of the South China Sea, area I: Gulf of Thailand and east coast of peninsular Malaysia, in *Proceedings of the First Technical Seminar on Marine Fishery Resources Survey in the South China Sea*, pp. 6–11, Southeast Asian Fish. Dev. Cent., Samutprakan, Thailand.
- Saadon, M. N., P. Rojana-anawat, and A. Snidvongs (1999), Physical characteristics of watermass in the South China Sea, Area I: Gulf of Thailand and east of peninsular Malaysia, in *First Technical Seminar on Marine Fishery Resources Survey in the South China Sea*, pp. 1–5, Southeast Asian Fish. Dev. Cent., Samutprakan, Thailand.
- Shaw, P. T., and S. Y. Chao (1994), Surface circulation in the South China Sea, *Deep Sea Res., Part I*, *41*(11/12), 1663–1683.
- Snidvongs, A. (1998), The oceanography of the Gulf of Thailand: Research and management policy, in *SEAPOL Integrated Studies of the Gulf of Thailand*, vol. 1, edited by D. M. Johnston, pp. 1–68, Southeast Asian Programme in Ocean Law, Policy and Management, Pakkred, Thailand.
- Snidvongs, A., and P. Sojisuporn (1999), Numerical simulations of the net current in the Gulf of Thailand under different monsoon regimes, in *Proceedings of the First Technical Seminar on Marine Fishery Resources Survey in the South China Sea*, pp. 54–85, Samutprakan Press, Samutprakan, Thailand.
- Stansfield, K., and C. Garrett (1997), Implications of the salt and heat budgets of the Gulf of Thailand, *J. Mar. Res.*, *55*, 935–963.
- Tang, D. L., I.-H. Ni, F. E. Müller-Karger, and Z. J. Liu (1998), Analysis of annual and spatial patterns of CZCS-derived pigment concentrations on the continental shelf of China, *Cont. Shelf Res.*, *18*, 1493–1515.
- Tang, D. L., I.-H. Ni, D. R. Kester, and F. E. Müller-Karger (1999), Remote sensing observation of winter phytoplankton blooms southwest of the Luzon Strait in the South China Sea, *Mar. Ecol. Prog. Ser.*, *191*, 43–51.
- Tang, D. L., H. Kawamura, and A. J. Luis (2002), Short-term variability of phytoplankton blooms associated with a cold eddy on the north-western Arabian Sea, *Remote Sens. Environ.*, *81*, 81–89.
- Tang, D. L., H. Kawamura, M. A. Lee, and T. V. Dien (2003), Seasonal and spatial distribution of chlorophyll a and water condition in the Gulf of Tonkin, South China Sea, *Remote Sens. Environ.*, *85*, 475–483.
- Tang, D. L., H. Kawamura, D. N. Hai, and W. Takahashi (2004a), Remote sensing oceanography of a harmful phytoplankton bloom (HAB) off the coast of southeastern Vietnam, *J. Geophys. Res.*, *109*, C03014, doi:10.1029/2003JC002045.
- Tang, D. L., H. Kawamura, T. V. Dien, and M. A. Lee (2004b), Offshore phytoplankton biomass increases and its oceanographic causes in the South China Sea, *Mar. Ecol. Prog. Ser.*, *268*, 31–41.
- Unoki, S. (1993), *Coastal Geophysical Oceanography* (in Japanese), 672 pp., Tokai Univ. Press, Tokyo.
- Walton, C. C., W. G. Pichel, J. E. Sapper, and D. A. May (1998), The development and operational application of nonlinear algorithms for the measurement of sea surface temperature with the NOAA polar-orbiting environmental satellite, *J. Geophys. Res.*, *103*, 27,999–28,012.
- Wentz, F. J., D. K. Smith, C. A. Mears, and C. L. Gentemann (2001), Advanced algorithms for QuikScat and SeaWinds/AMSR, paper presented at IGARSS ’01, NASA, Washington, D. C.
- Wyrtki, K. (1961), *Scientific Results of Marine Investigations of the South China Sea and the Gulf of Thailand 1959–1961*, *NAGA Rep.*, vol. 2, 195 pp., Scripps Inst. of Oceanogr., La Jolla, Calif.
- Yanagi, T., S. I. Sachoemar, T. Takao, and S. Fujiwara (2001), Seasonal variation of stratification in the Gulf of Thailand, *J. Oceanogr.*, *57*, 461–470.

L. Guan, Ocean Remote Sensing Institute, Ocean University of China, Qingdao 266003, China. (leiguan@orsi.ouc.edu.cn)

O. Isoguchi, H. Kawamura, F. Sakaida, and T. Shimada, Center for Atmospheric and Oceanic Studies, Graduate School of Science, Tohoku University, Sendai 9808578, Japan. (guchi@ocean.caos.tohoku.ac.jp; kamu@ocean.caos.tohoku.ac.jp; toki@ocean.caos.tohoku.ac.jp; shimada@ocean.caos.tohoku.ac.jp)

P. Shi and D. L. Tang, Laboratory for Tropical Marine Environmental Dynamics, South Chinese Sea Institute of Oceanology, Chinese Academy of Sciences, Guangzhou 510301, China. (pshi@scsio.ac.cn; lingzis@scsio.ac.cn)

W. Takahashi, Japan NUS Co., LTD, Tokyo 108-0022, Japan. (wataru@janus.co.jp)